

**FULL PAPER**

Propafenone analogue with additional H-bond acceptor group shows increased inhibitory activity on P-glycoprotein

Anna Cseke^{1*} | Theresa Schwarz^{1*} | Sankalp Jain^{1,2} | Simon Decker¹ | Kerstin Vogl¹ | Ernst Urban¹ | Gerhard F. Ecker¹ ¹Department of Pharmaceutical Chemistry, University of Vienna, Vienna, Austria²National Center for Advancing Translational Sciences, National Institutes of Health, Rockville, MD, USA**Correspondence**

Gerhard F. Ecker, Department of Pharmaceutical Chemistry, University of Vienna, Althanstrasse 14, 1090 Vienna, Austria.

Email: gerhard.f.ecker@univie.ac.at

Funding information

European Union's Horizon 2020 Research and Innovation Programme, Grant/Award Number: 681002 (EU-ToxRisk); Austrian Science Fund, Grant/Award Numbers: #F03502, SFB35

Abstract

P-glycoprotein (P-gp) is an ATP-dependent efflux pump that has a marked impact on the absorption, distribution, and excretion of therapeutic drugs. As P-gp inhibition can result in drug–drug interactions and altered drug bioavailability, identifying molecular properties that are linked to inhibition is of great interest in drug development. In this study, we combined chemical synthesis, in vitro testing, quantitative structure–activity relationship analysis, and docking studies to investigate the role of hydrogen bond (H-bond) donor/acceptor properties in transporter–ligand interaction. In a previous work, it has been shown that propafenone analogs with a 4-hydroxy-4-piperidine moiety exhibit a generally 10-fold higher P-gp inhibitory activity than expected based on their lipophilicity. Here, we specifically expanded the data set by introducing substituents at position 4 of the 4-phenylpiperidine moiety to assess the importance of H-bond donor/acceptor features in this region. The results suggest that indeed an H-bond acceptor, such as hydroxy and methoxy, increases the affinity by forming a H-bond with Tyr310.

KEYWORDS

inhibitor, molecular docking, P-glycoprotein, propafenone, quantitative structure–activity relationship

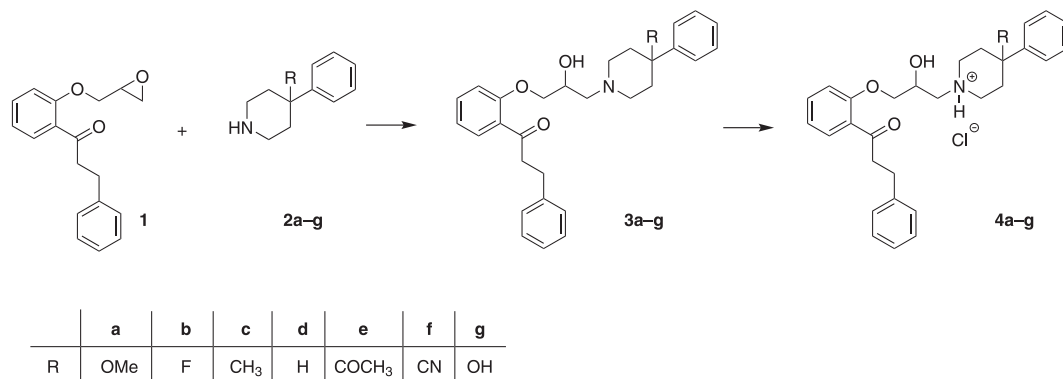
1 | INTRODUCTION

P-glycoprotein (P-gp) is an extensively studied efflux pump belonging to the ABC (ATP binding cassette) transporter superfamily.^[1] This transporter protein is integrated into the plasma membrane and uses the energy of adenosine triphosphate (ATP) hydrolysis to extrude a wide variety of substances from the intracellular to the extracellular compartment.^[2,3] In the human body, P-gp is physiologically expressed in tissues with barrier and/or excretory functions, including the liver, kidney, gastrointestinal tract and blood–brain

barrier, where it mediates the uptake and elimination of endogenous compounds and xenobiotics.^[4] In addition, overexpression of P-gp in cancerous cells has been recognized as a major cellular mechanism of multidrug resistance.^[5]

On the basis of its expression profile and broad substrate specificity, P-gp is involved in the absorption, distribution, and excretion of therapeutic drugs.^[6] Co-administration of a transported drug and a P-gp inhibitor can lead to elevated drug levels in the plasma and in the organs defended by blood–tissue barriers, which poses the risk of organ toxicity.^[7,8] On this account, both the US Food and Drug Administration (FDA) and the European Medicines Agency (EMA) recommend drug candidates to be routinely screened for their

*Anna Cseke and Theresa Schwarz contributed equally to this work.



SCHEME 1 Synthetic route to compounds **4a-g**

capacity to inhibit P-gp and the analogous breast cancer-resistant protein BCRP.^[9-11]

Over the past four decades, a considerable effort has been made to characterize the molecular basis of the interaction between P-gp and its inhibitors.^[12,13] Although within analogous sets of compounds (e. g. propafenone, tetrahydroisoquinoline, tariquidar and chalcone derivatives, alkaloids, and flavonoids), a clear structure-activity relationship (SAR) pattern was observed, a general and conclusive model is still missing.^[14-19] Numerous SAR studies suggested that there is a strong correlation between lipophilicity and P-gp inhibitory potency and that active compounds commonly possess at least one aromatic ring, a basic nitrogen atom, and several hydrophobic regions.^[12] Preference of P-gp toward lipophilic compounds can be explained by the widely accepted model of substrate transport, which proposes that P-gp extracts its ligands directly from the inner leaflet of the plasma membrane.^[20,21] In addition, ligand- and structure-based approaches suggest that hydrogen-bond (H-bond) acceptor properties are important for P-gp inhibitors.^[21,22]

Propafenone analogs are potent inhibitors of P-gp mediated drug efflux, exhibit a well-defined SAR pattern, and therefore, represent an excellent tool for investigating the molecular features triggering P-gp inhibition.^[23] Chiba et al.^[24] performed quantitative structure-activity relationship (QSAR) analyses on a series of highly related propafenone analogs and found a significant correlation between lipophilicity and inhibitory activity ($\log[1/EC_{50}]$). They also revealed that piperazine and piperidine analogous propafenone derivatives, which bear a 4-hydroxy-4-phenylpiperidine moiety, are generally 10-fold more active than equilipophilic compounds without a hydroxy group in position 4 of the piperidine ring. On the basis of the docking study of a small set of propafenone analogs into P-gp homology models, Klepsch et al.^[23] proposed the formation of an H-bond between the 4-hydroxy group of the 4-hydroxy-4-phenylpiperidine compound GPV062 (**4g**) and the Y310 moiety of P-gp. This additional H-bond could account for a stronger interaction with P-gp, and thus for the high relative activity of **4g** when compared to its calculated logP value ($EC_{50} = 0.07 \mu\text{M}$ and $\log P = 3.98$ ^[24]).^[25] In the present study, we further investigate the structural requirements for P-gp inhibition, focusing on the role of potential H-bond acceptors at

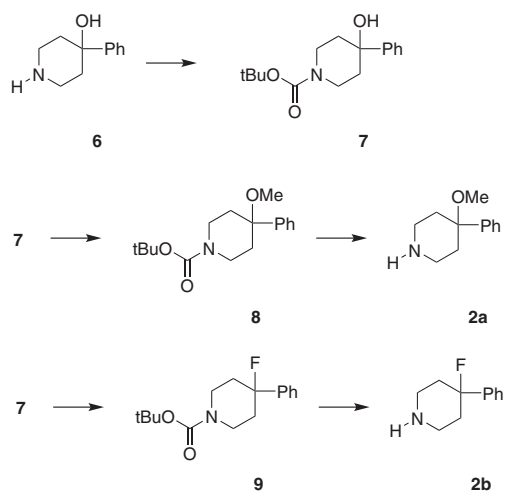
the 4-hydroxy-4-phenylpiperidine moiety. To this end, we synthesized six novel propafenone derivatives sharing the same scaffold with **4g**, but bearing varying functional groups in position 4 of the 4-phenylpiperidine substituent and tested their inhibitory activity on P-gp in vitro.

2 | RESULTS AND DISCUSSION

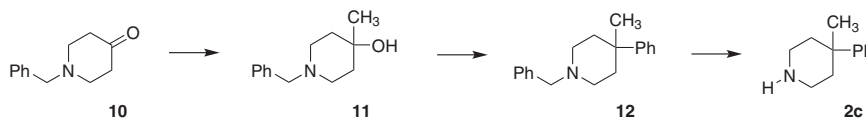
2.1 | Synthesis

The propafenone derivatives **3a-g** were synthesized by ring-opening reaction of oxirane **1** with appropriate substituted 4-phenylpiperidines **2a-g** and subsequently transformed to their hydrochlorides **4a-g**, as described previously by Chiba et al.^[24] (see Scheme 1). While 4-phenylpiperidines **2d-g** were commercially available, 4-phenylpiperidines **2a-c** were synthesized either from 4-hydroxy-4-phenylpiperidine **6** or 1-benzyl-4-piperidone **10** (see Schemes 2 and 3).

Following Barker et al.,^[26] the commercially acquired amine **6** was protected by Boc_2O to yield carbamate **7**. The free hydroxy group of **7** was activated using sodium hydride and methylated by methyl iodide to



SCHEME 2 Synthesis of 4-methoxy-4-phenylpiperidine and 4-fluoro-4-phenylpiperidine

SCHEME 3 Synthesis of 4-methyl-4-phenylpiperidine

give **8**. For deprotection of carbamates, the method of DeGoey et al.^[27] proved to give the best results. Thus, **8** was deprotected by HCl in dioxane to yield 4-methoxy-4-phenylpiperidine (**2a**).

Substitution of the hydroxy group in carbamate **7** by diethylaminosulfur trifluoride led to 4-fluoro-4-phenylpiperidine **11**. Deprotection of **11** by HCl in dioxane yielded 4-fluoro-4-phenylpiperidine (**2b**).

1-Benzyl-4-piperidone **10** was used as a starting material to synthesize 4-methyl-4-phenylpiperidine (**2c**). The addition of methyl-lithium to **10** gave 1-benzyl-4-methylpiperidin-4-ol (**11**), which was activated by aluminum chloride and reacted with benzene to yield the Friedel-Crafts alkylation product **12**. Finally, the protective group was removed by catalytic transfer hydrogenation in accordance with Salon et al.^[28] to give 4-methyl-4-phenylpiperidine (**2c**).

2.2 | In vitro studies

To evaluate the P-gp inhibitory activity of **4a-g**, the intracellular accumulation of daunorubicin in the P-gp overexpressing CCRF VCR1000 cells was measured by flow cytometry. As shown in Table 1, all compounds proved to be strong P-gp inhibitors with IC₅₀ values in the low nanomolar range (see Supporting Information for Figure S1 showing the dose-response curves). Among the new compounds, **4a** and **4d** showed the highest activity with IC₅₀ values of 0.03 ± 0.01 and 0.03 ± 0.00 μM, respectively, while the cyano derivative **4f** exhibited somewhat lower values (0.15 ± 0.04 μM). The IC₅₀ value of **4g** (0.05 ± 0.01 μM) was in good agreement with IC₅₀ values reported earlier for this compound (0.07,^[24] 0.06,^[29] and 0.06 μM^[30]), which demonstrates a high comparability with earlier experiments on series of propafenone analogs and thus allows to pool all compounds into one data set for subsequent QSAR analysis.

TABLE 1 Results of in vitro IC₅₀ evaluation of P-glycoprotein inhibition for the compounds **4a-g** (Scheme 1)

Compound	clogP ^a	R ^b	IC ₅₀ (μM) ^c
4a	4.65	OMe	0.03 ± 0.01
4b	4.90	F	0.06 ± 0.01
4c	5.61	CH ₃	0.05 ± 0.01
4d	5.31	H	0.03 ± 0.00
4e	5.13	COCH ₃	0.04 ± 0.01
4f	4.86	CN	0.15 ± 0.04
4g	4.01	OH	0.05 ± 0.01

^aCalculated partition coefficient logP(octanol/water); determined for newly synthesized compounds using the MarvinSketch software (ChemAxon).

^bSubstituent.

^cIC₅₀ values represent the mean ± standard deviation of *n* = 3 independent experiments performed in triplicate; IC₅₀ values were calculated as described in Section 4.

2.3 | QSAR analysis

As previously reported,^[24] a hydroxy group located at the 4-phenylpiperidine position of propafenone derivatives increases P-gp inhibitory activity, compared to other analogs with the same lipophilicity. Docking studies of analog **4g** into a protein homology model of P-gp indicated that this affinity increase is possibly due to an H-bond formed between the hydroxy group and Y310.^[23] However, as all four compounds synthesized by Chiba et al.^[24] bear a 4-phenyl-4-hydroxy moiety, other reasons than hydrogen bonding might be responsible for the affinity increase. Thus, to broaden the chemical space of the substituent at this position, we synthesized a set of compounds with different substituents on the 4-phenylpiperidine moiety. Substituents included the two H-bond acceptors methoxy and acetyl, as well as hydrogen, fluoro, methyl, and cyano, which are devoid of H-bonding capabilities.

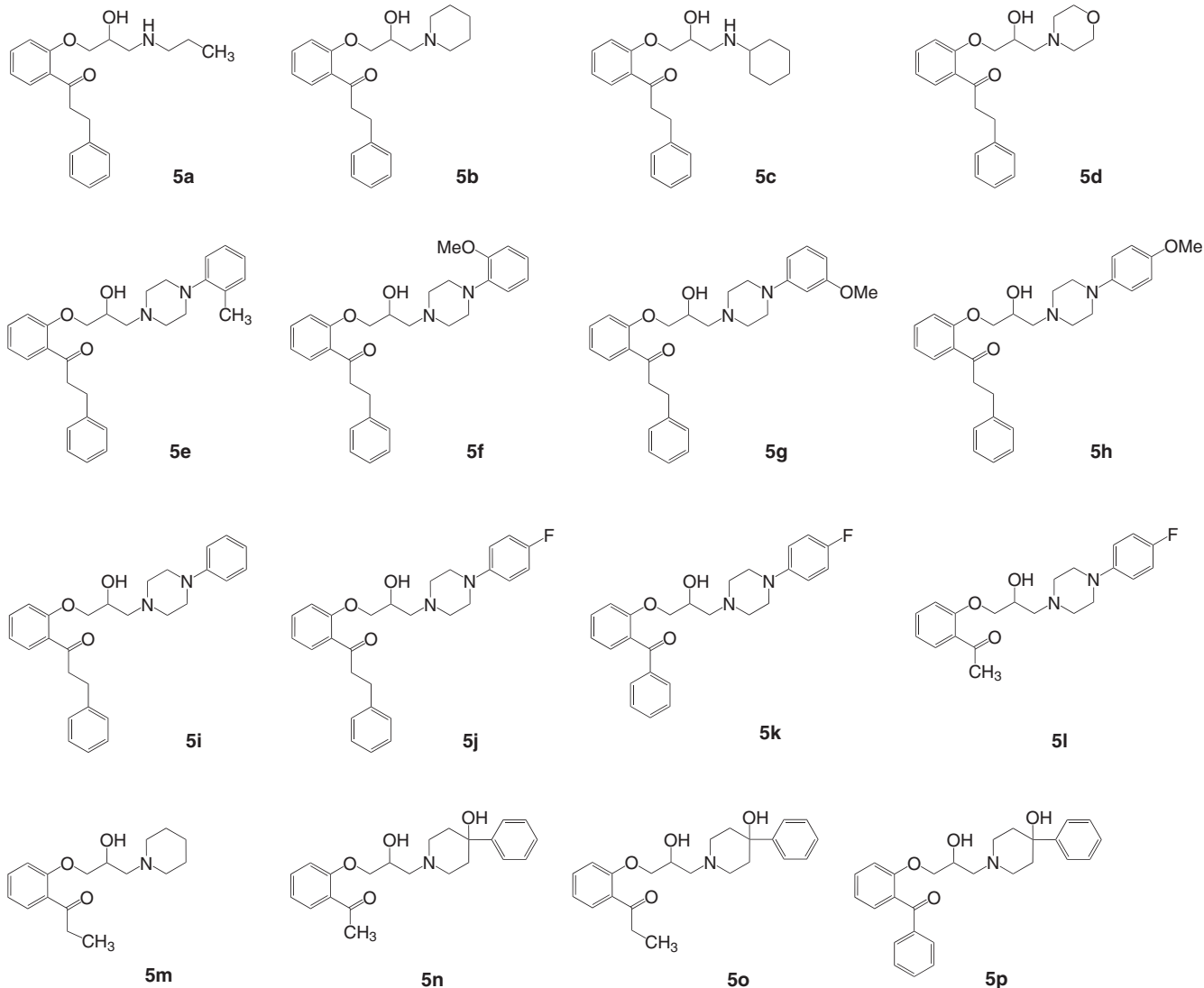
To evaluate the SAR of our newly synthesized compound set (**4a-f**) and **4g** in a broader context, we involved the propafenone analogs **5a-p** synthesized and characterized by Chiba et al.^[24] in the analysis (Table 2 and Scheme 4). A previous work showed that the activities (IC₅₀ values) of the sodium channel blocker propafenone and its analogs exhibit an excellent correlation with their octanol/water partition coefficient (logP value).^[31] As it is

TABLE 2 Calculated logP and IC₅₀ values of compounds **5a-p** (Scheme 4)^[24]

Compound	clogP ^a	IC ₅₀ (μM) ^b
5a	3.54	1.08
5b	3.89	0.68
5c	4.46	0.34
5d	2.82	3.75
5e	5.29	0.05
5f	4.62	0.11
5g	4.62	0.12
5h	4.62	0.18
5i	4.78	0.21
5j	4.83	0.14
5k	4.1	0.42
5l	2.73	3.84
5m	2.31	6.84
5n	1.73	2.83
5o	2.43	0.30
5p	3.63	0.19

^aCalculated partition coefficient logP(octanol/water) using the MarvinSketch software (ChemAxon).

^bIC₅₀ values experimentally determined by Chiba et al.^[24]



SCHEME 4 Chemical structures of compounds 5a-p^[24]

difficult to quantify the H-bonding capacity, we used an indicator variable for groups at the 4-piperidine position with H-bond donor or acceptor properties ($I = 1$; else $I = 0$) as a descriptor for multiple linear regression analysis:

$$pIC_{50} = 0.66(\pm 0.04)clogP + 0.73(\pm 0.10)I - 2.29(\pm 0.19),$$

$$(r^2 = 0.93; SD = 0.20; n = 23).$$

(1)

The results indicate that indeed an H-bond donor or acceptor in position 4 of the 4-piperidine is favorable for activity, which is apparent in the case of the 4-hydroxy-4-piperidines 5n-p and 4g, as well as for the 4-methoxy-4-piperidine derivative 4a (Figure 1). However, it is less pronounced for the acetyl analog 4e. This might be due to a less favorable positioning of the carboxy oxygen in the binding site. We therefore docked compound 4a and 4e into the binding pocket of a homology model of P-gp.

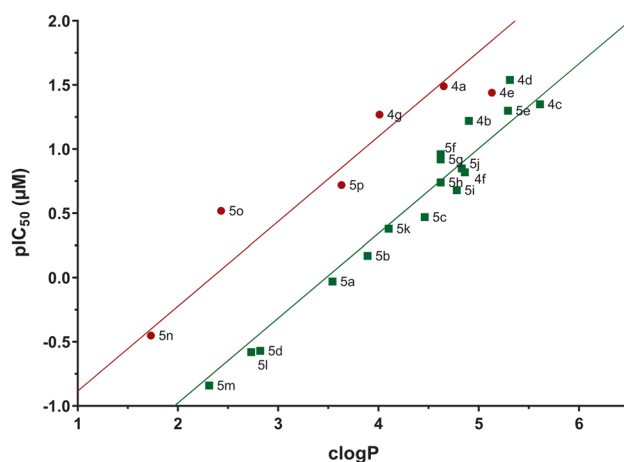


FIGURE 1 Correlation of P-glycoprotein inhibitory activity (expressed as pIC_{50} values) and calculated $\log P$ values. Propafenone analogs (\bullet) bearing and (\blacksquare) lacking a hydrogen-bond donor or acceptor group

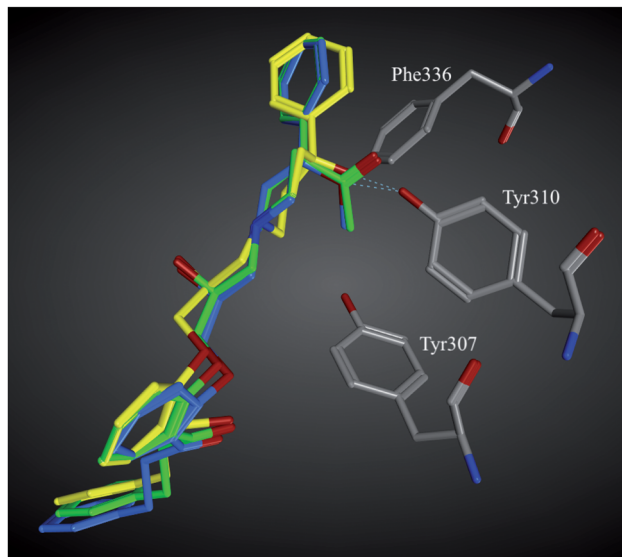


FIGURE 2 Interactions of the propafenone derivatives **4a** (blue), **4e** (green) and **4g** (yellow) with P-gp. The methoxy group of **4a** and the hydroxy group of **4g** formed an H-bond with Tyr310

2.4 | Molecular docking analysis

Due to the unavailability of the crystal structure of human P-gp, we used our recently published homology model^[32] for docking experiments. As can be seen from Figure 2, both the methoxy analog **4a** and the acetyl derivative **4e** are positioned in the same way as reported previously for the hydroxy compound **4g**.^[23] However, though the methoxy-oxygen is perfectly located for an H-bond with Tyr310, the position of the acetyl-oxygen is less suited for exploiting the full potential of a H-bond. This might be the reason for **4e** not perfectly fitting the regression line for 4-hydroxy-4-phenylpiperidines (IC_{50} measured, $0.04 \mu\text{M}$; IC_{50} predicted, $0.015 \mu\text{M}$). Further evidence could be obtained from binding affinity score predictions obtained from LigandScout 4.4,^[33] which provided a score of -46.27 for **4e**, and a slightly better score of -48.16 for **4a**. The hydroxy analog **4g** showed a binding affinity score of -45.67 , which is in line with the ranking observed in the biological experiments. These results thus strengthen the hypothesis that indeed hydrogen bonding with Tyr310 is the main driving factor for the increase of the $pIC_{50}/\log P$ ratio observed for 4-hydroxy/alkoxy-4-phenylpiperidine analogous propafenone derivatives.

3 | CONCLUSIONS

The ABC transporter P-gp is one of the driving molecular mechanisms for the development of multiple drug resistance in tumor therapy. Although thousands of compounds are known to inhibit the transporter, knowledge of the molecular basis of interaction for distinct inhibitor classes is still far from being complete. In the light of our studies on propafenone-type inhibitors of P-gp, we previously hypothesized the importance of an H-bond acceptor close to the

basic nitrogen atom of a 4-phenylpiperidine moiety. In this contribution, synthesis of a set of compounds with varied substituents at position 4 of the piperidine, followed by biological testing and ligand- and structure-based modeling studies further support this hypothesis. QSAR studies performed also once more outline the importance of lipophilicity as a main basic descriptor for activity, which might compensate for missing interaction features. Thus, SAR of compound series derived for P-gp should always be discussed in light of $pIC_{50}/\log P$ ratios rather than on pIC_{50} values alone.

4 | EXPERIMENTAL

4.1 | Chemistry

4.1.1 | General

All moisture-sensitive reactions were conducted in anhydrous solvents (Sigma-Aldrich) under dry argon atmosphere. All solvents and reagents were obtained from Sigma-Aldrich, ABCR, TCI, or Acros and used without further purification. 1-(2-((Oxiran-2yl)methoxy)-phenyl)-3-phenylpropan-1-one was synthesized following a literature procedure.^[24] All other reagents are commercially acquired and were used without further purification. Thin-layer chromatography (TLC) testings were done on Macherey–Nagel TLC sheets ALUGRAM Xtra SIL G/UV254. TLC silica gel 60 with fluorescent indicator UV₂₅₄ was visualized with UV-light (254 nm) or rather ninhydrin and/or Seebach stain. Silica gel 60 M 0.040–0.63 mm from Macherey–Nagel was used for flash chromatography to optimize yields. The InChI codes of the investigated compounds and the biological activity data are provided as Supporting Information Material.

4.1.2 | Nuclear magnetic resonance spectroscopy

¹H- and ¹³C-NMR-spectra were measured by Bruker Avance 500 Nuclear Magnetic Resonance spectrometer at 500 MHz using deuterated chloroform (CDCl₃) as the solvent. Chemical shifts are specified in parts per million (ppm) relative to tetramethylsilane and coupling constants (*J*) are given in Hertz (Hz). Multiplicities are described as s (singlet), brs (broad singlet), d (doublet), t (triplet), q (quadruplet), quin (quintuplet), septet or m (multiplet). Spectra were adjusted to the solvent signal of CDCl₃, $\delta(^1\text{H}) = 7.26 \text{ ppm}$ and $\delta(^{13}\text{C}) = 77.00 \text{ ppm}$, respectively. The ¹H- and ¹³C-NMR-spectra of newly synthesized compounds are given in the Supporting Information. For data of compounds **4g** and **5a-p**.^[24]

4.1.3 | High-resolution electrospray ionization mass spectrometry (HR-ESI-MS)

High-resolution mass spectra (HRMS) were obtained on a Bruker-Daltonics maXis HD ESI-Qq-TOF mass spectrometer using the direct

infusion. The ESI ion source was operated as follows: capillary voltage: 1.0 to 4.0 kV (individually optimized), nebulizer: 0.4 bar (N₂), dry gas flow: 4 l/min (N₂), and dry temperature: 200°C. Mass spectra were recorded in the range of *m/z* 50–1,550 in the positive-ion mode. The sum formulas were determined using Bruker Compass Data Analysis 4.2 based on the mass accuracy ($\Delta m/z \leq 2$ ppm) and isotopic pattern matching (SmartFormula algorithm).

4.1.4 | Synthesis of propafenone derivatives (general procedure)

Oxirane **1** and the 4-phenylpiperidine derivatives were dissolved in MeOH under argon. The mixture was stirred at reflux for 2 hr. Then the solvent was removed under reduced pressure.

1-(2-(2-Hydroxy-3-(4-methoxy-4-phenylpiperidine-1-yl)propoxy)-phenyl)-3-phenylpropan-1-one (**3a**)

Phenylpiperidine **2a** (200 mg; 1.05 mmol; 1 eq.) and oxirane **1** (290 mg; 1.03 mmol; 1.02 eq.) in methanol (5 ml) gave after chromatographic purification (silica gel, DCM, MeOH, conc. NH₃ 200 + 0 + 1 to 200 + 5 + 1) 400 mg **3a**, yellow oil, 82% yield. ¹H-NMR (500 MHz, CDCl₃): δ = 1.93 (m, 1H), 1.95 (m, 1H), 2.00 (m, 1H), 2.01 (m, 1H), 2.37 (t, *J* = 11.0 Hz, 1H), 2.49 (m, 1H), 2.53 (m, 2H), 2.68 (td, *J* = 11.3, 3.0 Hz, 1H), 2.75 (d, *J* = 11.0 Hz, 2H), 2.97 (s, 3H), 3.04 (t, *J* = 7.7 Hz, 2H), 3.38 (td, *J* = 7.8, 3.3 Hz, 2H), 4.08 (m, 1H), 4.09 (m, 2H), 6.97 (d, *J* = 8.2 Hz, 1H), 7.02 (t, *J* = 7.6 Hz, 1H), 7.18 (t, *J* = 6.9 Hz, 1H), 7.27 (m, 4H), 7.30 (m, 1H), 7.38 (m, 2H), 7.41 (m, 2H), 7.45 (t, *J* = 7.9 Hz, 1H), and 7.72 (d, *J* = 7.9 Hz, 1H) ppm. ¹³C-NMR (125 MHz, CDCl₃): δ = 30.27 (CH₂), 34.70 (CH₂), 34.86 (CH₂), 45.55 (CH₂), 47.85 (CH₂), 49.38 (CH₃), 50.76 (CH₂), 60.66 (CH₂), 65.21 (CH), 70.91 (CH₂), 75.19 (Cq), 112.58 (CH), 120.97 (CH), 125.85 (CH), 125.94 (2C, CH), 127.26 (CH), 128.25 (Cq), 128.35 (2C, CH), 128.39 (4C, CH), 130.44 (CH), 133.46 (CH), 141.63 (Cq), 144.38 (Cq), 157.81 (Cq), and 201.37 (Cq) ppm. HRMS (ESI): calcd for C₃₀H₃₅NO₄ *m/z* 474.2639 [M+H]⁺, found *m/z* 474.2641 [M+H]⁺.

1-(2-(3-(4-Fluoro-4-phenylpiperidine-1-yl)-2-hydroxypropoxy)-phenyl)-3-phenylpropan-1-one (**3b**)

Phenylpiperidine **2b** (124 mg; 0.54 mmol; 1 eq.) and oxirane **1** (324 mg; 1.15 mmol; 1.5 eq.) in methanol (8 ml) gave after chromatographic purification (silica gel, DCM, MeOH, conc. NH₃ 200 + 0 + 1 to 200 + 5 + 1) 70.9 mg **3b**, yellow oil, 27% yield. ¹H-NMR (500 MHz, CDCl₃): δ = 1.98 (m, 1H), 1.99 (m, 1H), 2.08 (m, 1H), 2.13 (m, 1H), 2.35 (t, *J* = 11.5 Hz, 1H), 2.56 (m, 2H), 2.58 (m, 1H), 2.68 (t, *J* = 10.9 Hz, 1H), 2.82 (d, *J* = 11.0 Hz, 1H), 3.05 (t, *J* = 7.9 Hz, 2H), 3.38 (m, 2H), 4.09 (m, 1H), 4.10 (m, 2H), 6.98 (d, *J* = 8.2 Hz, 1H), 7.03 (t, *J* = 7.4 Hz, 1H), 7.18 (t, *J* = 6.8 Hz, 1H), 7.26 (m, 4H), 7.32 (m, 1H), 7.40 (m, 4H), 7.47 (t, *J* = 7.3 Hz, 1H), and 7.73 (d, *J* = 7.9 Hz, 1H) ppm. ¹³C-NMR (125 MHz, CDCl₃): δ = 30.30 (CH₂), 36.80 (d, *J*(¹³C–¹⁹F) = 21.6 Hz, CH₂), 37.11 (d, *J*(¹³C–¹⁹F) = 20.9 Hz, CH₂), 45.70 (CH₂), 47.82 (CH₂), 50.98 (CH₂), 60.78 (CH₂), 65.40 (CH), 70.85 (CH₂), 112.63 (CH), 121.05 (CH), 123.89 (d, *J*(¹³C–¹⁹F) = 9.2 Hz, 2C, CH), 125.93 (CH), 127.64 (CH),

128.22 (Cq), 128.39 (6C, CH), 128.89 (2C, CH), 130.49 (CH), 133.51 (CH), 141.65 (Cq), 144.19 (d, *J*(¹³C–¹⁹F) = 20.9 Hz, Cq), 157.80 (Cq), and 201.21 (Cq) ppm. HRMS (ESI): calcd for C₂₉H₃₃FNO₃ *m/z* 462.2439 [M+H]⁺, found *m/z* 462.2439 [M+H]⁺.

1-(2-(2-Hydroxy-3-(4-methyl-4-phenylpiperidine-1-yl)propoxy)-phenyl)-3-phenylpropan-1-one (**3c**)

Phenylpiperidine **2c** (95 mg; 0.54 mmol, 1 eq.) and oxirane **1** (124 mg; 0.54 mmol, 1 eq.) in methanol (8 ml) gave after chromatographic purification (silica gel, DCM, MeOH, conc. NH₃ 200 + 0 + 1 to 200 + 5 + 1) 136 mg **3c**, yellow oil, 94% yield. ¹H-NMR (500 MHz, CDCl₃): δ = 1.23 (s, 3H), 1.76 (m, 2H), 2.12 (m, 2H), 2.27 (m, 1H), 2.34 (m, 1H), 2.43 (m, 2H), 2.54 (m, 1H), 2.64 (m, 1H), 3.02 (t, *J* = 7.8 Hz, 2H), 3.35 (t, *J* = 8.1 Hz, 2H), 4.00 (m, 1H), 4.04 (m, 1H), 4.08 (m, 1H), 6.95 (d, *J* = 8.2 Hz, 1H), 7.01 (t, *J* = 7.5 Hz, 1H), 7.16 (m, 1H), 7.21 (m, 1H), 7.23 (m, 4H), 7.34 (m, 2H), 7.35 (m, 2H), 7.44 (td, *J* = 7.8, 2.0 Hz, 1H), and 7.71 (dd, *J* = 7.7, 1.8 Hz, 1H) ppm. ¹³C-NMR (125 MHz, CDCl₃): δ = 29.68 (CH₂), 30.26 (CH₂), 36.00 (Cq), 37.08 (2C, CH₂), 45.58 (CH₂), 50.29 (2C, CH₂), 60.85 (CH₂), 65.06 (CH), 70.91 (CH₂), 112.55 (CH), 120.96 (CH), 125.72 (3C, CH), 125.86 (CH), 128.21 (Cq), 128.34 (4C, CH), 128.40 (2C, CH), 130.42 (CH), 133.47 (CH), 141.62 (Cq), 148.70 (Cq), 157.78 (Cq), and 201.30 (Cq) ppm. HRMS (ESI): calcd for C₃₀H₃₆NO₃ *m/z* 458.2690 [M+H]⁺, found *m/z* 458.2690 [M+H]⁺.

1-(2-(2-Hydroxy-3-(4-phenylpiperidine-1-yl)propoxy)phenyl)-3-phenylpropan-1-one (**3d**)

Phenylpiperidine **2d** (200 mg; 1.24 mmol; 1 eq.) and oxirane **1** (360 mg; 1.26 mmol; 1 eq.) in methanol (5 ml) gave after chromatographic purification (silica gel, DCM, MeOH, conc. NH₃ 200 + 0 + 1 to 200 + 5 + 1) 190 mg **3d**, white to pale yellow oil, 35% yield. ¹H-NMR (500 MHz, CDCl₃): δ = 1.72 (m, 1H), 1.77 (m, 1H), 1.80 (m, 1H), 1.82 (m, 1H), 1.93 (t, *J* = 11.8 Hz, 1H), 2.31 (td, *J* = 11.5, 2.4 Hz, 2H), 2.48 (m, 1H), 2.50 (m, 1H), 2.52 (m, 1H), 2.76 (d, *J* = 11.3 Hz, 1H), 2.99 (d, *J* = 11.7 Hz, 1H), 3.04 (t, *J* = 7.7 Hz, 2H), 3.38 (td, *J* = 7.9, 3.6 Hz, 2H), 4.07 (m, 2H), 4.11 (m, 1H), 6.97 (d, *J* = 8.2 Hz, 1H), 7.02 (t, *J* = 7.6 Hz, 1H), 7.18 (t, *J* = 6.8 Hz, 1H), 7.23 (m, 1H), 7.24 (m, 2H), 7.25 (m, 2H), 7.28 (m, 2H), 7.33 (t, *J* = 7.6 Hz, 2H), 7.45 (t, *J* = 7.7 Hz, 1H), and 7.73 (d, *J* = 7.9 Hz, 1H) ppm. ¹³C-NMR (125 MHz, CDCl₃): δ = 30.30 (CH₂), 33.34 (CH₂), 33.69 (CH₂), 42.33 (CH), 45.73 (CH₂), 52.65 (CH₂), 55.99 (CH₂), 61.13 (CH₂), 65.23 (CH), 70.86 (CH₂), 112.55 (CH), 120.99 (CH), 125.89 (CH), 126.25 (CH), 126.79 (2C, CH), 128.17 (Cq), 128.38 (2C, CH), 128.41 (2C, CH), 128.46 (2C, CH), 130.48 (CH), 133.52 (CH), 141.71 (Cq), 146.07 (Cq), 157.92 (Cq), and 201.33 (Cq) ppm. HRMS (ESI): calcd for C₂₉H₃₄NO₃ *m/z* 444.2533 [M+H]⁺, found *m/z* 444.2536 [M+H]⁺.

1-(2-(3-(4-Acetyl-4-phenylpiperidine-1-yl)-2-hydroxypropoxy)-phenyl)-3-phenylpropan-1-one (**3e**)

Phenylpiperidine **2e** (254 mg; 1.06 mmol; 1 eq.) and oxirane **1** (300 mg; 1.06 mmol; 1 eq.) in methanol (8 ml) gave after chromatographic purification (silica gel, DCM, MeOH, conc. NH₃ 200 + 0 + 1 to 200 + 5 + 1) 303 mg **3e**, yellow oil, 57% yield. ¹H-NMR (500 MHz, CDCl₃): δ = 1.92 (s, 3H), 2.02 (m, 2H), 2.16 (t, *J* = 10.4 Hz, 1H), 2.39

(m, 1H), 2.43 (m, 2H), 2.45 (m, 2H), 2.47 (m, 1H), 2.75 (m, 1H), 3.03 (t, $J = 7.9$ Hz, 2H), 3.35 (td, $J = 8.2, 3.9$ Hz, 2H), 4.02 (m, 1H), 4.04 (m, 2H), 6.95 (d, $J = 8.2$ Hz, 1H), 7.01 (t, $J = 7.6$ Hz, 1H), 7.17 (t, $J = 7.1$ Hz, 1H), 7.23 (m, 2H), 7.26 (m, 2H), 7.28 (m, 1H), 7.30 (m, 2H), 7.38 (t, $J = 7.7$ Hz, 2H), 7.44 (t, $J = 7.9$ Hz, 1H), and 7.70 (d, $J = 7.6$ Hz, 1H) ppm. ^{13}C -NMR (125 MHz, CDCl_3): $\delta = 25.61$ (CH_3), 30.25 (CH_2), 32.79 (CH_2), 32.91 (CH_2), 45.52 (CH_2), 50.11 (CH_2), 51.61 (CH_2), 54.43 (Cq), 60.60 (CH_2), 65.23 (CH), 70.84 (CH_2), 112.62 (CH), 121.00 (CH), 125.78 (CH), 126.34 (2C, CH), 128.24 (5C, CH und Cq), 127.27 (CH), 128.95 (2C, CH), 130.42 (CH), 133.45 (CH), 141.68 (2C, Cq), 157.81 (Cq), 201.27 (Cq), and 209.29 (Cq) ppm. HRMS (ESI): calcd for $\text{C}_{31}\text{H}_{36}\text{NO}_4$ m/z 486.2639 $[\text{M}+\text{H}]^+$, found m/z 486.2638 $[\text{M}+\text{H}]^+$.

1-(2-(2-Hydroxy-3-(2-(3-phenylpropanoyl)phenoxy)propyl)-4-phenylpiperidine-4-carbonitrile (3f)

Phenylpiperidine **2f** (236 mg; 1.06 mmol; 1 eq.) and oxirane **1** (300 mg; 1.06 mmol; 1 eq.) in methanol (8 ml) gave after chromatographic purification (silica gel, DCM, MeOH, conc. NH_3 200 + 0 + 1 to 200 + 10 + 1) 69 mg **3f**, yellow oil, 13% yield. ^1H -NMR (500 MHz, CDCl_3): $\delta = 2.09$ (td, 4H), 2.44 (td, $J = 12.1, 2.1$ Hz, 1H), 2.59 (m, 2H), 2.74 (m, 2H), 2.99 (d, $J = 12.0$ Hz, 1H), 3.05 (t, $J = 8.5$ Hz, 2H), 3.37 (m, 2H), 4.08 (m, 1H), 4.09 (m, 2H), 6.97 (d, $J = 8.5$ Hz, 1H), 7.03 (t, $J = 7.4$ Hz, 1H), 7.18 (t, $J = 7.3$ Hz, 1H), 7.25 (m, 2H), 7.28 (m, 2H), 7.36 (t, $J = 7.4$ Hz, 1H), 7.43 (m, 2H), 7.46 (m, 1H), 7.50 (d, $J = 7.9$ Hz, 2H), and 7.73 (dd, $J = 7.6, 1.2$ Hz, 1H) ppm. ^{13}C -NMR (125 MHz, CDCl_3): $\delta = 30.29$ (CH_2), 36.45 (CH_2), 36.69 (CH_2), 42.44 (Cq), 45.61 (CH_2), 49.36 (CH_2), 52.31 (CH_2), 60.50 (CH_2), 65.54 (CH), 70.78 (CH_2), 112.77 (CH), 121.12 (CH), 121.79 (CN), 125.55 (2C, CH), 125.95 (2C, CH), 128.21 (Cq), 128.40 (2C, CH), 128.43 (2C, CH), 129.08 (2C, CH), 130.47 (CH), 133.52 (CH), 139.78 (Cq), 141.64 (Cq), 157.83 (Cq), and 201.16 (Cq) ppm. HRMS (ESI): calcd for $\text{C}_{30}\text{H}_{33}\text{N}_2\text{O}_3$ m/z 469.2486 $[\text{M}+\text{H}]^+$, found m/z 469.2485 $[\text{M}+\text{H}]^+$.

4.1.5 | Synthesis of hydrochlorides (general procedure)

The propafenone derivatives were dissolved in ether under argon then HCl in ether (2 M) was added and stirred for 1 hr at room temperature. The mixture was filtered, washed with ether, and dried.

1-(2-(2-Hydroxy-3-(4-methoxy-4-phenylpiperidine-1-yl)propoxy)-phenyl)-3-phenylpropan-1-one hydrochloride (4a)

3a (100 mg; 0.21 mmol; 1 eq.), ether (6 ml), HCl in ether (0.21 ml; 2 M; 2 eq.) gave **4a** (73 mg white to gray powder, 61% yield). HRMS (ESI): calcd for $\text{C}_{30}\text{H}_{36}\text{NO}_4$ m/z 474.2639 $[\text{M}+\text{H}]^+$, found m/z 474.2642 $[\text{M}+\text{H}]^+$.

1-(2-(3-(4-Fluoro-4-phenylpiperidine-1-yl)-2-hydroxypropoxy)-phenyl)-3-phenylpropan-1-one hydrochloride (4b)

3b (71.0 mg; 0.15 mmol; 1 eq.), ether (8 ml), HCl in ether (0.15 ml; 2 M; 2 eq.) gave **4b** (39.5 mg white powder, 56% yield). HRMS (ESI): calcd for $\text{C}_{29}\text{H}_{33}\text{FNO}_3$ m/z 462.2439 $[\text{M}+\text{H}]^+$, found m/z 462.2442 $[\text{M}+\text{H}]^+$.

1-(2-(2-Hydroxy-3-(4-methyl-4-phenylpiperidine-1-yl)propoxy)-phenyl)-3-phenylpropan-1-one hydrochloride (4c)

3c (90.0 mg; 0.20 mmol; 1 eq.), ether (8 ml), HCl in ether (0.20 ml; 2 M; 2 eq.) gave **4c** (79 mg white powder, 88% yield). HRMS (ESI): calcd for $\text{C}_{30}\text{H}_{36}\text{NO}_3$ m/z 458.2690 $[\text{M}+\text{H}]^+$, found m/z 458.2694 $[\text{M}+\text{H}]^+$.

1-(2-(2-Hydroxy-3-(4-phenylpiperidine-1-yl)propoxy)phenyl)-3-phenylpropan-1-one hydrochloride (4d)

3d (55.0 mg; 0.21 mmol; 1 eq.), ether (8 ml), HCl in ether (0.12 ml; 2 M; 2 eq.) gave **4d** (49.6 mg white powder, 90% yield). HRMS (ESI): calcd for $\text{C}_{29}\text{H}_{34}\text{NO}_3$ m/z 444.2533 $[\text{M}+\text{H}]^+$, found m/z 444.2533 $[\text{M}+\text{H}]^+$.

1-(2-(3-(4-Acetyl-4-phenylpiperidine-1-yl)-2-hydroxypropoxy)-phenyl)-3-phenylpropan-1-one hydrochloride (4e)

3e (240 mg; 0.48 mmol; 1 eq.), ether (8 ml), HCl in ether (0.50 ml; 2 M; 2 eq.) gave **4e** (225 mg white to gray powder, 88% yield). HRMS (ESI): calcd for $\text{C}_{31}\text{H}_{36}\text{NO}_4$ m/z 486.2639 $[\text{M}+\text{H}]^+$, found m/z 486.2640 $[\text{M}+\text{H}]^+$.

1-(2-Hydroxy-3-(2-(3-phenylpropanoyl)phenoxy)propyl)-4-phenylpiperidine-4-carbonitrile hydrochloride (4f)

3f (69.0 mg; 0.13 mmol; 1 eq.), ether (8 ml), HCl in ether (0.14 ml; 2 M; 2 eq.) gave **4f** (35 mg white to gray powder, 51% yield). HRMS (ESI): calcd for $\text{C}_{30}\text{H}_{33}\text{N}_2\text{O}_3$ m/z 469.2486 $[\text{M}+\text{H}]^+$, found m/z 469.2486 $[\text{M}+\text{H}]^+$.

4.1.6 | Synthesis of substituted 4-phenylpiperidines

tert-Butyl 4-hydroxy-4-phenylpiperidine-1-carboxylate (7)

4-Hydroxy-4-phenylpiperidine **6** (15 g, 84.6 mmol; 1 eq.) and di-tert-butyl dicarbonate (20.25 g, 93.15 mmol; 1.1 eq.) were dissolved in DCM (450 ml) under argon and stirred at room temperature for 2 hr. Then saturated aqueous NaHCO_3 solution was added. The aqueous phase was washed three times with DCM and the organic phases were dried over Na_2SO_4 , filtered and concentrated. Yield: 24.53 g **7**, yellow to light brown oil, 105% (was used without further purification). ^1H -NMR (500 MHz, CDCl_3): $\delta = 1.48$ (s, 9H), 1.73 (d, $J = 12.6$ Hz, 2H), 2.00 (td, $J = 13.2, 4.7$ Hz, 2H), 3.24 (td, $J = 12.9, 2.1$ Hz, 2H), 4.03 (dt, $J = 13.2, 2.0$ Hz, 2H), 7.29 (t, $J = 7.6$ Hz, 1H), 7.37 (t, $J = 7.6, 2\text{H}$), and 7.48 (d, $J = 7.9$ Hz, 2H) ppm. ^{13}C -NMR (125 MHz, CDCl_3): $\delta = 28.46$ (3C, CH_3), 30.08 (2C, CH_2), 39.84 (2C, CH_2), 71.53 (Cq), 79.49 (Cq), 124.40 (2C, CH), 127.26 (CH), 128.47 (2C, CH), 147.94 (Cq), and 154.87 (Cq) ppm.

tert-Butyl 4-methoxy-4-phenylpiperidine-1-carboxylate (8)

tert-Butyl 4-hydroxy-4-phenylpiperidine-1-carboxylate **7** (2 g, 7.2 mmol; 1 eq.) was dissolved in THF (60 ml) under argon. Sodium hydride (0.18 g, 7.5 mmol; 1.04 eq.) was added portionwise. The mixture was stirred at room temperature for 1 hr. Methyl iodide

(0.64 ml, 10.8 mmol; 1.5 eq.) was added and the reaction was stirred overnight at room temperature. On the next day, more sodium hydride (0.15 g, 6.3 mmol, 0.88 eq.) and methyl iodide (0.33 ml; 5.2 mmol, 0.72 eq.) were added, and the mixture was stirred overnight at room temperature again. Saturated aqueous NaCl solution was added to the reaction, and the aqueous phase was washed three times with EtOAc. The organic phases were dried over Na₂SO₄, filtered, and concentrated. Yield: 2.06 g **8**, yellow oil, 98% yield. ¹H-NMR (500 MHz, CDCl₃): δ = 1.47 (s, 9H), 1.84 (td, *J* = 13.2, 4.4 Hz, 2H), 2.01 (d, *J* = 13.2 Hz, 2H), 2.98 (s, 3H), 3.17 (t, *J* = 12.5 Hz, 2H), 3.97 (d, *J* = 12.9 Hz, 2H), 7.26–7.31 (m, 1H), and 7.34–7.40 (m, 4H) ppm. ¹³C-NMR (125 MHz, CDCl₃): δ = 28.45 (3C, CH₃), 34.52 (2C, CH₂), 39.60 (2C, CH₂), 49.87 (CH₃), 75.62 (Cq), 79.38 (Cq), 125.91 (2C, CH), 127.34 (CH), 128.34 (2C, CH), 144.19 (Cq), and 154.95 (Cq) ppm.

4-Methoxy-4-phenylpiperidine (2a)

tert-Butyl 4-methoxy-4-phenylpiperidine-1-carboxylate **8** (2.06 g, 7.07 mmol; 1 eq.) was dissolved in dioxane and HCl (4.7 ml, 4 M; 2.5 eq.) and stirred for 4 hr under argon. More HCl (1 ml, 6 M; 0.85 eq.) was added and the mixture was stirred overnight at room temperature. Then saturated aqueous NaHCO₃ solution was added. The aqueous phase was washed three times with EtOAc and the organic phases were dried over Na₂SO₄, filtered, and concentrated.^[27] Yield: 580 mg **2a**, yellow oil, 45% yield. ¹H-NMR (500 MHz, CDCl₃): δ = 1.94 (td, *J* = 12.5, 4.2 Hz, 2H), 2.04 (d, *J* = 13.6 Hz, 2H), 2.97 (s, 3H), 2.97–3.06 (m, 2H), 3.11 (t, *J* = 11.8 Hz, 2H), 7.27 (t, *J* = 7.3 Hz, 1H), 7.36 (t, *J* = 7.6 Hz, 2H), and 7.39 (d, *J* = 7.9 Hz, 2H) ppm. ¹³C-NMR (50 MHz, CDCl₃): δ = 33.24 (2C, CH₂), 40.77 (2C, CH₂), 49.74 (CH₃), 74.78 (Cq), 125.79 (2C, CH), 127.51 (CH), 128.48 (2C, CH), and 143.40 (Cq) ppm. HRMS (ESI): calcd for C₁₂H₁₈NO *m/z* 192.1383 [M+H]⁺, found *m/z* 192.1382 [M+H]⁺.

tert-Butyl-4-fluoro-4-phenylpiperidine-1-carboxylate (9)

tert-Butyl-4-hydroxy-4-phenylpiperidine-1-carboxylate **7** (2.00 g; 7.2 mmol; 1.2 eq.) in DCM (25 ml) was cooled to –78°C under argon. A solution of diethylaminosulfur trifluoride (0.81 ml; 6.1 mmol; 1 eq.) in DCM (3 ml) was added dropwise. The mixture was stirred between –70 and –90°C for 1 hr. Then it was warmed to room temperature and stirred for another 30 min. Saturated aqueous NaHCO₃ solution was added, and the organic phases were washed with brine. Then, 3-chloroperoxybenzoic acid (0.375 g; 2.2 mmol) was added and the reaction was stirred for 30 min at room temperature. Saturated aqueous NaHCO₃ solution was added and the organic phase was washed with saturated aqueous NaHCO₃ solution, water, and brine. The organic phases were dried with Na₂SO₄, tested for peroxide and concentrated. Yield: 1.56 g **9**, light brown oil, 77% yield. ¹H-NMR (500 MHz, CDCl₃): δ = 1.49 (d, *J* = 3.8 Hz, 9H), 1.74 (d, *J* = 12.6 Hz, 2H), 1.92–2.07 (m, 2H), 3.21 (dtd, *J* = 35.7, 12.9, 2.2 Hz, 2H), 4.07 (dd, *J* = 42.2, 13.6 Hz, 2H), 7.27–7.34 (m, 1H), 7.34–7.39 (m, 2H), 7.43 (dd, *J* = 50.9, 7.4 Hz, 2H) ppm. ¹³C-NMR (50 MHz, CDCl₃): δ = 28.43 (3C, CH₃), 36.50 (d, *J*(¹³C–¹⁹F) = 23.2 Hz, 2C, CH₂), 39.68 (2C, CH₂), 79.71

(Cq), 94.23 (d, *J*(¹³C–¹⁹F) = 174.5 Hz, Cq), 123.81 (d, *J*(¹³C–¹⁹F) = 1.9 Hz, 2C, CH), 127.68 (d, *J*(¹³C–¹⁹F) = 1.3 Hz, CH), 128.39 (d, *J*(¹³C–¹⁹F) = 1.0 Hz, 2C, CH), 144.01 (d, *J*(¹³C–¹⁹F) = 21.3 Hz, Cq), and 154.78 (Cq) ppm.

4-Fluoro-4-phenylpiperidine (2b)

Hydrogen chloride solution (0.97 ml; 2 M) was added to *tert*-butyl-4-fluoro-4-phenylpiperidine-1-carboxylate **9** (0.20 g, 0.72 mmol) in dioxane (5 ml) under argon and stirred for 4 hr at room temperature. Because NMR showed there was no reaction, hydrogen chloride solution (5 ml; 2 M) was added and stirred overnight at room temperature. Afterward, the mixture was concentrated. Yield: 0.17 g **2b**, dark brown, olive oil, 86% yield. ¹H-NMR (500 MHz, CDCl₃): δ = 2.16 (dd, *J* = 14.2, 8.5 Hz, 2H), 2.66 (dt, *J* = 38.3, 13.3 Hz, 2H), 3.38 (d, *J* = 7.9 Hz, 2H), 3.58 (d, *J* = 10.7 Hz, 2H), 7.29–7.44 (m, 5H) and 9.65 (brs, 1H) ppm. ¹³C-NMR (125 MHz, CDCl₃): δ = 33.30 (d, *J*(¹³C–¹⁹F) = 22.7 Hz, 2C, CH₂), 40.36 (2C, CH₂), 92.15 (d, *J*(¹³C–¹⁹F) = 177.8 Hz, Cq), 123.65 (d, *J*(¹³C–¹⁹F) = 9.2 Hz, 2C, CH), 128.30 (CH), 128.65 (2C, CH), and 141.99 (d, *J*(¹³C–¹⁹F) = 21.4 Hz, Cq) ppm.

1-Benzyl-4-methylpiperidine-4-ol (11)

Methylolithium (30.4 ml, 48.6 mmol) was added dropwise to a solution of 1-benzyl-4-piperidone **10** (5 ml; 27 mmol) in THF (40 ml) at –78°C and stirred for 1 hr 30 min. Ether and water were added and the phases were separated. The aqueous phase was extracted with diethyl ether, combined with the organic phase, dried with Na₂SO₄ and concentrated. The product was purified by flash chromatography with petroleum ether and EtOAc 3 + 1 to 1 + 2. Yield: 2.4 g **11**, dark brown oil, 43% yield. ¹H-NMR (500 MHz, CDCl₃): δ = 1.24 (s, 3H), 1.58 (d, *J* = 13.2 Hz, 2H), 1.70 (dd, *J* = 13.4, 10.9, 3.3 Hz, 2H), 2.39 (t, *J* = 9.9, 2H), 2.55–2.64 (m, 2H), 3.54 (s, 2H), and 7.24–7.37 (m, 5H) ppm. ¹³C-NMR (125 MHz, CDCl₃): δ = 29.90 (CH₃), 38.55 (2C, CH₂), 49.60 (2C, CH₂), 62.99 (CH₂), 67.83 (Cq), 127.04 (CH), 128.19 (2C, CH), 129.26 (2C, CH), and 138.08 (Cq) ppm.

1-Benzyl-4-methyl-4-phenylpiperidine (12)

1-Benzyl-4-methylpiperidine-4-ol **11** (1.0 g; 4.9 mmol) and aluminum chloride (3.24 g; 24.3 mmol) were dissolved in benzene (21 ml) under argon and stirred at reflux for 18 hr. Benzene (10 ml) was added again and the mixture was poured cautiously into ice water. The pH of the aqueous phase was adjusted to 11–12 by the addition of aqueous sodium hydroxide solution (6 M) at a temperature of 0°C. The aqueous phase was extracted with EtOAc, the organic fractions were combined, dried over Na₂SO₄ and concentrated. The product was purified by flash chromatography with petroleum ether and diethyl ether 19 + 1 to 1 + 1. Yield: 0.550 g **12**, light brown oil, 43% yield. ¹H-NMR (500 MHz, CDCl₃): δ = 1.22 (s, 3H), 1.74–1.85 (m, 2H), 2.10–2.20 (m, 2H), 2.36–2.46 (m, 2H), 2.47–2.57 (m, 2H), 3.47 (s, 2H), 7.19 (t, *J* = 7.1 Hz, 1H), 7.22–7.27 (m, 1H), and 7.29–7.37 (m, 8H) ppm. ¹³C-NMR (125 MHz, CDCl₃): δ = 29.39 (CH₃), 36.12 (Cq), 37.00 (2C, CH₂), 50.25 (2C, CH₂), 63.37 (CH₂), 125.48 (CH), 125.82 (2C, CH), 126.86 (CH), 128.13 (2C, CH), 128.25 (2C, CH), 129.16 (2C, CH), 138.67 (Cq), and 149.23 (Cq) ppm. HRMS (ESI): calcd for C₂₄H₂₆N *m/z* 328.2060 [M+H]⁺, found *m/z* 328.2062 [M+H]⁺.

4-Methyl-4-phenylpiperidine (2c)

Methanolic formic acid solution (12 ml; 4.4 wt%; 5.5 eq.) was freshly prepared and added to 1-benzyl-4-methyl-4-phenylpiperidine **12** (550 mg; 2.07 mmol; 1 eq.) and Pd on activated carbon (350 mg; 10 wt%) and stirred overnight. The mixture was filtered over celite and washed with MeOH, water, DCM, and MeOH, and concentrated. The aqueous residue was washed three times with DCM, dried over Na₂SO₄ and concentrated. Yield: 0.307 g **2c**, light brown oil, 85% yield. ¹H-NMR (500 MHz, CDCl₃): δ = 1.25 (s, 3H), 1.66–1.79 (m, 2H), 2.02–2.14 (m, 2H), 2.78–2.89 (m, 2H), 2.90–2.99 (m, 2H), 7.14–7.24 (m, 1H), and 7.29–7.41 (m, 4H) ppm. ¹³C-NMR (125 MHz, CDCl₃): δ = 29.64 (CH₃), 36.60 (Cq), 38.07 (2C, CH₂), 42.91 (2C, CH₂), 125.60 (CH), 125.67 (2C, CH), 128.35 (2C, CH), and 149.30 (Cq) ppm. HRMS (ESI): calcd for C₁₂H₁₈N m/z 176.1434 [M+H]⁺, found m/z 176.1433 [M+H]⁺.

4.2 | In vitro inhibition studies

4.2.1 | Materials

Rosewell Park Memorial Institute-1640 (RPMI-1640) cell culture media was purchased from Thermo Fisher Scientific (Waltham, MA). Supplements for cell culture, including fetal bovine serum (FBS), the antibiotics penicillin and streptomycin, as well as vincristine for selection of the CCRF VCR1000 cells were obtained from Sigma-Aldrich (St. Louis, MO). The fluorescent substrate daunorubicin as well as verapamil, DMSO, phosphate-buffered saline (PBS) and all compounds used for RPMI buffer preparation were also purchased from Sigma-Aldrich.

4.2.2 | Cell culture

The human T-lymphoblast cell line CCRF VCR1000, overexpressing P-gp, was generated by stepwise selection of CCRF-CEM cells in the vincristine-containing medium^[34] and was kindly provided by V. Gekeler (Altana-Pharma AG, formerly Byk-Gulden, Konstanz, Germany). CCRF VCR1000 cells were cultured in RPMI-1640 medium containing 20% FBS and were treated regularly with vincristine (1 µg/ml) for 72 hr, followed by centrifugation (300 g, 5 min, RT) and resuspension in a normal cell culture medium. Cells were maintained at 37°C in an atmosphere containing 5% CO₂ with 95% relative humidity.

4.2.3 | Steady-state daunorubicin accumulation experiments

For P-gp inhibition studies, the steady-state accumulation of daunorubicin (3 µM) was performed as previously described,^[14] optimized to a 96-well plate format. Cells were harvested, pelleted (300 g, 5 min, 4°C), and diluted to a concentration of 12 × 10⁶ cells/ml in RPMI (10 mM Hepes, 120 mM NaCl, 5 mM KCl, 0.4 mM MgCl₂, 0.04 mM CaCl₂, 10 mM glucose, 10 mM NaHCO₃, 5 mM Na₂HPO₄, pH 7.4 with NaOH). For each data point, 15 µl of cell suspension was preincubated

for 5 min at 37°C with 15 µl of 2% DMSO in RPMI alone (DMSO control) or containing different concentrations of test compound solutions. Incubation was done by placing the 96-well plate (nerbe plus GmbH, Winsen/Luhe, Germany) into an Eppendorf ThermoMixer® C device (Eppendorf, Hamburg, Germany). Thereafter, cells were loaded with 30 µl of daunorubicin, for 30 min at 37°C, to reach a final daunorubicin concentration of 3 µM. The final DMSO concentration was 0.5%. Loading was stopped by chilling the cells on watery ice for 5 min followed by the addition of 120 µl ice-cold PBS. Cells were pelleted (300 g, 5 min, 4°C), the supernatant was aspirated and cell pellet was resuspended in 120 µl ice-cold PBS. Until measurement cells were kept on ice and in the dark. Immediately before cell fluorescence measurement by flow cytometry (MACSQuant, Miltenyi Biotec GmbH, Bergisch Gladbach, Germany), 40 µl of DAPI solution (4 µg/ml in PBS) was added to gate out dead cells. Cells were kept at 4°C during measurement. Verapamil (100 µM) was included as a positive control for P-gp inhibition. The background fluorescence of the cell suspension was measured in the presence of 0.5% DMSO.

4.2.4 | IC₅₀ value measurements and calculations

Flow cytometry data were analyzed using FlowJo software (Tree Star, Ashland, OR). IC₅₀ apparent values were estimated measuring eight different compound concentrations and performing nonlinear regression analyses (GraphPad Prism 6; “log(Agonist) vs. response–Variable slope” GraphPad Software, La Jolla, CA), for which the following equation was used:

$$Y = \text{Bottom} + \frac{\text{Top} - \text{Bottom}}{1 + 10^{(\text{Log}(\text{IC}_{50 \text{ apparent}}) - X) \cdot \text{Hillslope}}}, \quad (2)$$

where X is the log of compound concentration, Y is the response in fluorescent intensity units, “bottom” and “top” are the lower and the higher plateaus of the nonlinear fit curve, respectively, and Hillslope is a factor that describes the steepness of the curve.

To correct for the dependency of IC₅₀ apparent values on the expression level of P-gp and the pump-leak kinetics as reviewed by Stein,^[35] the final IC₅₀ values were calculated using the following Equation:

$$\text{IC}_{50} = \text{IC}_{50 \text{ apparent}} \cdot \frac{\text{Bottom}}{\text{Top}}, \quad (3)$$

where “bottom” and “top” are the lower and the higher plateaus of the nonlinear fit curve, respectively, and therefore they refer to the fluorescence intensity at zero and infinite inhibitor concentration, respectively.^[36] The mean IC₅₀ values ± standard deviations given were calculated from three independent experiments for each compound.

4.3 | Calculation of lipophilicity and QSAR studies

The logP values were calculated using the “consensus” method of the MarvinSketch software (ChemAxon).^[37] The performance of the

“consensus” method was verified on a set of 19 propafenone derivatives whose distribution coefficient was experimentally determined by Chiba et al.,^[31] using high-performance liquid chromatography (HPLC). The experimentally obtained and the calculated values were in good agreement ($r = 0.98$). QSAR studies carried out comprised multiple linear regression analyses performed in MS Excel.

4.4 | Molecular docking analysis

To further understand the association between the activity of the compounds (**4a** and **4e**) and the molecular structure, we performed molecular docking studies. The LigPrep module of Schrödinger Suite^[38] was used to generate the correct protonation states for the ligands, which were then used for the docking studies. The OPLS_2005 force field was applied for the minimization of the structures and different ionization states were generated by adding or removing protons from the ligand at a target pH of 7.0 ± 2.0 using Epik, version 3.1.^[39,40] Tautomers were also generated for each ligand. To generate stereoisomers, the information on chirality from the input file for each ligand was retained as is for the entire calculation. This resulted in a data set of 12 ligands. Due to unavailability of the crystal structure of P-gp, we used the homology model published by Jain et al.^[32] The protein was prepared using the Protein Preparation Wizard of the Schrödinger Suite (2015).^[41,42] Hydrogen atoms were added, and optimal protonation states and ASN/GLN/HIS flips were determined. The binding site was defined as the complete transmembrane region. Docking was performed using the genetic algorithm-based docking program GOLD.^[43,44] All side-chains were kept rigid and the ligand was treated flexible by performing 100 genetic algorithm runs per molecule. The implemented Gold scoring function, GoldScore, was used for the evaluation of the complexes. Top scored poses were then inspected for the presence of protein–ligand interactions as reported by Klepsch et al.^[23] and successively a final pose for each ligand (**4a** and **4e**) was selected.

ACKNOWLEDGMENTS

The authors thank V. Gekeler for providing the CCRF VCR1000 cells. They also thank D. Dobusch for performing the HRMS analysis. They wish to acknowledge the helpful discussions provided by M. Grandits and E. Heiß and thank ChemAxon for kindly providing them with their software. This project has received funding from the European Union’s Horizon 2020 research and innovation programme under grant agreement no. 681002 (EU-ToxRisk) and the Austrian Science Fund (SFB35, #F03502).

CONFLICT OF INTERESTS

The authors declare that there are no conflicts of interests.

ORCID

Anna Cseke  <http://orcid.org/0000-0002-1801-0317>

Gerhard F. Ecker  <http://orcid.org/0000-0003-4209-6883>

REFERENCES

- [1] E. E. Chufan, H.-M. Sim, S. V. Ambudkar *ABC Transporters and Cancer*, Vol. 125 (Eds: J. D. Schuetz, T. Ishikawa), Academic Press, New York, NY **2015**, Ch. 3.
- [2] F. J. Sharom, *Essays Biochem.* **2011**, *50*, 161. <https://doi.org/10.1042/bse0500161>
- [3] R. Silva, V. Vilas-Boas, H. Carmo, R. J. Dinis-Oliveira, F. Carvalho, M. de Lourdes Bastos, F. Remião, *Pharmacol. Ther.* **2015**, *149*, 1. <https://doi.org/10.1016/j.pharmthera.2014.11.013>
- [4] J. König, F. Müller, M. F. Fromm, *Pharmacol. Rev.* **2013**, *65*, 944. <https://doi.org/10.1124/pr.113.007518>
- [5] Z. Chen, T. Shi, L. Zhang, P. Zhu, M. Deng, C. Huang, T. Hu, L. Jiang, *Cancer Lett.* **2016**, *370*, 153. <https://doi.org/10.1016/j.canlet.2015.10.010>
- [6] J. Keogh, B. Hagenbuch, C. Rynn, B. Stieger, G. Nicholls *Role and Importance in ADME and Drug Development*, Vol. 1 (Eds: G. Nicholls, K. Youdim), Royal Society Of Chemistry, Cambridge, UK **2016**, Ch. 1.
- [7] D. Balayssac, N. Authier, A. Cayre, F. Coudore, *Toxicol. Lett.* **2005**, *156*, 319. <https://doi.org/10.1016/j.toxlet.2004.12.008>
- [8] F. Montanari, G. F. Ecker, *Adv. Drug Deliv. Rev.* **2015**, *86*, 17. <https://doi.org/10.1016/j.addr.2015.03.001>
- [9] Food and Drug Administration, Clinical drug interaction studies—Study design, data analysis, and clinical implications guidance for industry, Silver Spring, MD, **2017**. <https://www.fda.gov/downloads/Drugs/GuidanceComplianceRegulatoryInformation/Guidances/UCM581965.pdf> (accessed: November, 2018).
- [10] European Medicines Agency, Guideline on the investigation of drug interactions, London, UK, **2012**. https://www.ema.europa.eu/documents/scientific-guideline/guideline-investigation-drug-interactions_en.pdf (accessed: November, 2018).
- [11] M. Lund, T. S. Petersen, K. P. Dalhoff, *Drugs* **2017**, *77*, 859. <https://doi.org/10.1007/s40265-017-0729-x>
- [12] H. Liu, Z. Ma, B. Wu, *Xenobiotica* **2013**, *43*, 1018. <https://doi.org/10.3109/00498254.2013.791003>
- [13] R. Callaghan, *Biochem. Soc. Trans.* **2015**, *43*, 995. <https://doi.org/10.1042/BST20150131>
- [14] T. Schwarz, F. Montanari, A. Cseke, K. Wlcek, L. Visvader, S. Palme, P. Chiba, K. Kuchler, E. Urban, G. F. Ecker, *ChemMedChem* **2016**, *11*, 1380. <https://doi.org/10.1002/cmdc.201500592>
- [15] M. Contino, S. Guglielmo, M. G. Perrone, R. Giampietro, B. Rolando, A. Carrieri, D. Zaccaria, K. Chegav, V. Borio, C. Riganti, K. Zabielska-Koczywaś, N. A. Colabufo, R. Fruttero, *MedChemComm* **2018**, *9*, 862. <https://doi.org/10.1039/c8md00075a>
- [16] I. K. Pajeva, M. Hanl, M. Wiese, K. Steggemann, F. Marighetti, M. Wiese, *ChemMedChem* **2013**, *8*, 1701. <https://doi.org/10.1002/cmdc.201300233>
- [17] X. Ma, M. Hu, H. Wang, J. Li, *Eur. J. Med. Chem.* **2018**, *159*, 381. <https://doi.org/10.1016/j.ejmech.2018.09.061>
- [18] S. B. Syed, M. S. Coumar, *Curr. Top. Med. Chem.* **2016**, *16*, 2484. <https://doi.org/10.2174/1568026616666160212123814>
- [19] A. Ferreira, S. Pousinho, A. Fortuna, A. Falcão, G. Alves, *Phytochem. Rev.* **2015**, *14*, 233. <https://doi.org/10.1007/s11101-014-9358-0>
- [20] F. J. Sharom, *Front. Oncol.* **2014**, *4*, 41. <https://doi.org/10.3389/fonc.2014.00041>
- [21] Y. Xu, E. Egidio, X. Li-Blatter, R. Müller, G. Merino, S. Bernèche, A. Seelig, *Biochemistry* **2015**, *54*, 6195. <https://doi.org/10.1021/acs.biochem.5b00649>

- [22] P. Matsson, J. M. Pedersen, U. Norinder, C. A. S. Bergström, P. Artursson, *Pharm. Res.* **2009**, *26*, 1816. <https://doi.org/10.1007/s11095-009-9896-0>
- [23] F. Klepsch, P. Chiba, G. F. Ecker, *PLoS Comput. Biol.* **2011**, *7*, e1002036. <https://doi.org/10.1371/journal.pcbi.1002036>
- [24] P. Chiba, M. Hitzler, E. Richter, M. Huber, C. Tmej, E. Giovagnoni, G. Ecker, *Quant Struct-Act Relat* **1997**, *16*, 361. <https://doi.org/10.1002/qsar.19970160502>
- [25] E. E. Chufan, K. Kapoor, S. V. Ambudkar, *Biochem. Pharmacol.* **2016**, *101*, 40. <https://doi.org/10.1016/j.bcp.2015.12.007>
- [26] O. Barker, J. Bentley, M. G. Bock, T. Cain, P. Chovatia, J. R. Dod, F. Eustache, L. Gleave, J. Hargrave, A. Heifetz, R. Law, A. Raoof, D. Willows (Novartis AG, Switzerland), WO2012035023A1, **2012**.
- [27] D. A. DeGoey, W. M. Kati, C. W. Hutchins, P. L. Donner, A. C. Krueger, J. T. Randolph, C. E. Motter, L. T. Nelson, S. V. Patel, M. A. Matulenko, R. G. Keddy, T. K. Jinkerson, Y. Gao, D. Liu, J. K. Pratt, T. W. Rockway, C. J. Maring, D. K. Hutchinson, C. A. Flentge, R. Wagner, M. D. Tufano, D. A. Betebenner, K. Sarris, K. R. Woller, S. H. Wagaw, J. C. Califano, W. Li, D. D. Caspi, M. E. Bellizzi, W. A. Carroll (Abbott Laboratories, USA), WO2012051361A1, **2012**.
- [28] J. A. Salon, T. M. Laz, R. Nagorny, A. E. Wilson (Synaptic Pharmaceutical Corporation, USA), WO2002002744A2, **2002**.
- [29] T. Langer, M. Eder, R. D. Hoffmann, P. Chiba, G. F. Ecker, *Arch. Pharm.* **2004**, *337*, 317. <https://doi.org/10.1002/ardp.200300817>
- [30] G. Ecker, M. Huber, D. Schmid, P. Chiba, *Mol. Pharmacol.* **1999**, *56*, 791.
- [31] P. Chiba, G. Ecker, D. Schmid, J. Drach, B. Tell, S. Goldenberg, V. Gekeler, *Mol. Pharmacol.* **1996**, *49*, 1122.
- [32] S. Jain, M. Grandits, G. F. Ecker, *Eur. J. Pharm. Sci.* **2018**, *122*, 134. <https://doi.org/10.1016/j.ejps.2018.06.022>
- [33] LigandScout, version 4.4., Inte:Ligand Software Development and Consulting GmbH, Vienna, Austria, **2019**.
- [34] R. Boer, V. Gekeler, W. R. Ulrich, P. Zimmermann, W. Ise, A. Schödl, S. Haas, *Eur. J. Cancer* **1996**, *32*, 857. [https://doi.org/10.1016/0959-8049\(95\)00661-3](https://doi.org/10.1016/0959-8049(95)00661-3)
- [35] W. D. Stein, *Physiol. Rev.* **1997**, *77*, 545. <https://doi.org/10.1152/physrev.1997.77.2.545>
- [36] T. Litman, T. Skovsgaard, W. D. Stein, *J. Pharmacol. Exp. Ther.* **2003**, *307*, 846. <https://doi.org/10.1124/jpet.103.056960>
- [37] ChemAxon, MarvinSketch version 18.10, ChemAxon Ltd., Budapest, Hungary, **2018**.
- [38] Schrödinger Release 2015-1: LigPrep, version 3.3, Schrödinger, LLC, New York, NY, **2015**.
- [39] J. C. Shelley, A. Cholleti, L. L. Frye, J. R. Greenwood, M. R. Timlin, M. Uchimaya, *J. Comput.-Aided Mol. Des.* **2007**, *21*, 681. <https://doi.org/10.1007/s10822-007-9133-z>
- [40] J. R. Greenwood, D. Calkins, A. P. Sullivan, J. C. Shelley, *J. Comput.-Aided Mol. Des.* **2010**, *24*, 591. <https://doi.org/10.1007/s10822-010-9349-1>
- [41] G. M. Sastry, M. Adzhigirey, T. Day, R. Annabhimoju, W. Sherman, *J. Comput.-Aided Mol. Des.* **2013**, *27*, 221. <https://doi.org/10.1007/s10822-013-9644-8>
- [42] Schrödinger Release 2015-1: Maestro, version 10.1, Schrödinger, LLC, New York, NY, **2015**.
- [43] M. L. Verdonk, J. C. Cole, M. J. Hartshorn, C. W. Murray, R. D. Taylor, *Proteins Struct. Funct. Bioinf.* **2003**, *52*, 609. <https://doi.org/10.1002/prot.10465>
- [44] G. Jones, P. Willett, R. C. Glen, A. R. Leach, R. Taylor, *J. Mol. Biol.* **1997**, *267*, 727. <https://doi.org/10.1006/jmbi.1996.0897>

SUPPORTING INFORMATION

Additional supporting information may be found online in the Supporting Information section.

How to cite this article: Cseke A, Schwarz T, Jain S, et al. Propafenone analogue with additional H-bond acceptor group shows increased inhibitory activity on P-glycoprotein. *Arch Pharm Chem Life Sci.* 2020;e1900269. <https://doi.org/10.1002/ardp.201900269>